






Heavy-oxide glasses with superior mechanical assets for nonlinear fiber applications in the mid-infrared

CLÉMENT STRUTYNSKI,¹ FLORIAN CALZAVARA,¹ THÉO GUERINEAU,¹  LAURA LOI,² ROMAIN LABERDESQUE,² JEAN-MICHEL RAMPNOUX,³ STEEVE MORENCY,⁴ YANNICK LEDEMI,⁴ YANNICK PETIT,¹ MARC DUSSAUZE,⁵ FRÉDÉRIC DÉSÉVÉDAVY,⁶ FRÉDÉRIC SMEKTALA,⁶  SYLVAIN DANTO,¹ LIONEL CANIONI,²  YOUNES MESSADDEQ,⁴ EVELYNE FARGIN,¹ AND THIERRY CARDINAL^{1,*}

¹ Institut de Chimie de la Matière Condensée de Bordeaux (ICMCB), CNRS, UMR 5026, International Associated Laboratory (LIA) LuMAQ, University of Bordeaux, 33608 Pessac, France

² Center for Intense Lasers and Applications (CELIA), CNRS, CEA, UMR 5107, International Associated Laboratory (LIA) LuMAQ, University of Bordeaux, 351 Cours de la Libération, 33405 Talence, France

³ Laboratoire Ondes et Matière d'Aquitaine (LOMA), UMR 5798, CNRS- University of Bordeaux, 33400 Talence, France

⁴ Centre d'Optique, Photonique et Laser (COPL), International Associated Laboratory (LIA) LuMAQ: Université Laval, 2375 rue de la Terrasse, Québec, QC, G1V 0A6, Canada

⁵ Institute of Molecular Science (ISM), UMR 5255 CNRS, International Associated Laboratory (LIA) LuMAQ, University of Bordeaux, 33405 Talence, France

⁶ Laboratoire Interdisciplinaire Carnot de Bourgogne (ICB), UMR CNRS 6303, University de Bourgogne Franche-Comté, 21078 Dijon, France

*thierry.cardinal@icmcb.cnrs.fr

Abstract: The ability to produce robust fiber-based integrated optical systems operating over a wide spectral domain (UV to mid-infrared), is one of today's key challenges in photonics. This work reports on the production of crystal-free, light guiding fibers from rich Ga₂O₃ oxide-based glass compositions. These materials show optical transmission extending from ultraviolet wavelengths (~0.280 μm) up to 6 μm in the IR for millimeter length scale while exhibiting relatively high vitreous transition temperatures (~735 °C), nonlinear optical properties and improved surface micro-hardness. This combination of superior thermal, mechanical and optical properties represents a promising alternative for the development of robust fibers operating in the visible up to the 3–5 μm window.

© 2021 Optical Society of America under the terms of the [OSA Open Access Publishing Agreement](#)

1. Introduction

With their endlessly tailorable structures, optical fibers have revolutionized the way light can be manipulated. Their technological maturity has rapidly grown over time, and they now offer an essential framework for the engineering of ever more innovative sensors, laser sources and numerous other photonic devices. Still today, power scaling as well as extension of the spectral range of operation of fiber-based systems keep on driving highly motivated studies. Great efforts are for instance dedicated to the development and improvement of IR transmitting glasses suitable for optical fiber drawing [1]. Several vitreous systems such as chalcogenides, fluorides, tellurites and germanates, have emerged as strong alternatives to silica [2], offering new opportunities in various application fields. Yet, fibered systems based on these materials are still not able to reach silica's performances in terms of power sustainability, mechanical properties

or chemical stability. For instance, chalcogenide glasses suffer from poor thermal resistance limiting their use for high-energy applications despite being the most adequate materials in terms of nonlinear responses and transmission in the IR [3,4]. Fluorides are currently the most mature non-silica glasses for technological purposes. They possess low optical losses in the fiber form ($\sim 1 \text{ dB.km}^{-1}$) as well as greatly advanced integration (connectors, Bragg gratings, splicing) and functionalization (end caps) possibilities [5,6]. However, their performances are impaired by poor corrosion resistance, recrystallization during splicing, and low mechanical strength in general.

During the past fifteen years, significant efforts were devoted to the development of a fiberizable oxide-based alternative to silica, which could offer wide transparency from the UV to the Mid-IR with reinforced thermal and mechanical properties. In particular, lead and bismuth-free BGG (20 BaO - 10 Ga₂O₃ - 70 GeO₂) compositions were patented [7]. These gallo-germanate oxide glasses offer a wide optical transparency, ranging from $\sim 0.280 \mu\text{m}$ in the UV up to $\sim 6 \mu\text{m}$ in the Mid-IR, high glass transition temperature ($T_g \sim 700 \text{ }^\circ\text{C}$) and superior mechanical properties and damage threshold. [8,9] It has moreover been demonstrated recently that interesting $2 \mu\text{m}$ emission can be obtained from modified BGG glass fibers [10]. Most of the works dedicated to those vitreous materials however studied multi-component compositions possessing GaO_{3/2}/GeO₂ ratio less than 1:2, with gallium oxide behaving like an intermediate [10,11]. Ga₂O₃ possesses a relatively low phonon energy (500 cm^{-1}) as compared to other heavy oxides which contributes to extending transmission at longer wavelengths, as IR transmission edge is mainly limited by the species in the glass exhibiting the highest phonon energy. Its incorporation also enables to reinforce surface hardness or to modulate the refractive index. Despite their numerous assets, few studies have been devoted to fiber fabrication from glasses in which gallium oxide is acting as a network former. This is mainly due to the high complexity of the elaboration route of lead or bismuth-free gallate compositions which needs fast quenching techniques such as levitation [12,13] and that does not meet fiber preform fabrication requirements. Here experimental results concerning the fabrication of glass fibers obtained by the standard preform-to-fiber method in the GaO_{3/2} - GeO_{1/2} - BaO system stabilized with lanthanides (LaO_{3/2} or YO_{3/2}) are presented. Glasses with GaO_{3/2}/GeO_{1/2} ratio up to 3:2 were produced and successfully drawn into tens-of-meters-long fiber samples. Our study presents, for the first time, accurate nonlinear optical measurements and Raman gain on rich gallium oxide environmental-friendly glass compositions compatible with standard fiber fabrication technology.

2. Experimental section

2.1. Glass synthesis and fiber drawing

The glass performs are fabricated by the standard melt-quenching technique. High purity raw materials Ga₂O₃ (99.999%), GeO₂ (99.999%), BaCO₃ (99.997%), La₂O₃ (99.99%) and Y₂O₃ (99.99%) are weighted in adequate proportions and placed together in a platinum crucible. The mix is heated up to $1550 \text{ }^\circ\text{C}$ in an electric furnace and melted for 12 hours. Then, the melt is rapidly quenched by pouring it in a cylindric steel mold preheated at $\sim T_g - 50 \text{ }^\circ\text{C}$. The glass sample is subsequently annealed at $T_g - 10 \text{ }^\circ\text{C}$ for 5 hours. Finally, the temperature is slowly ramped down ($2 \text{ }^\circ\text{C.min}^{-1}$) to room temperature. A typical glass rod is 50 mm long, has a 10 mm diameter and weights approximately 40 g. The absence of crystallization were controlled by XRD, confirming, within the accuracy of the technique, that the glass was at least 98% amorphous. The fabricated preform is then thermally drawn under argon gas flow (2 L.min^{-1}) into fibers using a dedicated 3 meters high drawing tower. The rod is placed in the furnace and heated up to its softening temperature at a rate of $10 \text{ }^\circ\text{C.min}^{-1}$. After the fiber drawing is initiated, the preform is slowly fed (1 mm.min^{-1}) into the furnace while the drawing parameters are continuously monitored in order to produce fibers with a controlled diameter ranging from $125 \text{ to } 175 \mu\text{m} \pm 1 \mu\text{m}$.

2.2. Physical properties

The characteristic temperatures, namely the glass transition (T_g) were determined with ± 5 °C accuracy using Differential Thermal Analysis (DTA). Curves for ~ 100 mg glass samples were recorded under ambient atmosphere between 20–1000 °C at a heating rate of 10 °C.min⁻¹. The T_g was taken at the inflection point of the endotherm, as obtained by taking the first derivative of the DTA curve.

The Knoop microhardness (HK) measurements were carried out using a Leica WMHT Auto Apparatus equipped with a CCD camera. A charge of 100 g (= 0.981 N) was applied during 10 seconds in this case. Ten measurements performed all over the sample surface were averaged in order to obtain the microhardness of the glass.

The UV-Visible-NIR transmission spectra of the glass were recorded in the 0.2 μm - 3.3 μm range using an Agilent Cary 5000 UV-Vis-NIR spectrometer. Transmission in the Mid-IR was collected using a Bruker FTIR between 3 μm to 7 μm . The measurements were carried out on few millimeters (2 mm) optically polished glass slabs.

Optical losses measurements of single-index fibers were carried out using the cutback method on several meters-long samples. A fibered tungsten source is injected into the gallate fiber. Transmission of the sample is then recorded between 0.2 μm - 1.1 μm by using a fibered spectrometer Avantes AvaSpec-ULS4096CL-EVO while the transmission in the Infrared between 1.0 μm - 2.4 μm is recorded using a Fourier Transform Infrared (FTIR) spectrometer (NICOLET 6700). Additionally, the optical losses were measured at a discrete laser wavelength at 1.310 μm using the cutback method on a ~ 3 meters long fiber. A few mW 1.310 μm laser source is coupled into the gallate fiber by the means of a silica objective (x20 and 0,32 NA). The output power is then measured for different sample lengths using a power-meter with μW sensitivity.

The Raman gain cross-section was calculated from spontaneous scattering spectra measured in in VV (vertical polarization for the excitation and the analysis) configuration using a micro-Raman setup. The excitation wavelength used was 0.632 μm . The Laser beam is focused on the glass samples with a 100x objective with 0.9 numerical aperture and the signal is collected in backscattering configuration. Scaling corrections with respect to a well-known standard sample (fused silica) were implemented. They take into account variation in the solid-angle and Fresnel reflection as described elsewhere [14].

Third harmonic generation (THG) experiments were carried out using a femtosecond oscillator (TPulse200 from Amplitude Système, central wavelength 1.030 μm , mean power 2.4 W, 9.2 MHz repetition rate, 390 fs pulse duration (FWHM)), focused across the polished glass interface with a Olympus air objective (20x – NA 0.75). THG traces were recorded at different positions of the glass sample and averaged for both the glass under study and a reference Silica sample, to allow for the calibration of the THG signals. THG trace processing was carefully conducted so as to extract the cubic nonlinearity [15], which specifically requires to know accurately the involved refractive indices. A spectroscopic phase modulated ellipsometric measurement had thus been performed with an UVISEL apparatus (HORIBA Jobin-Yvon) to determine the refractive index n of the GGBLaY glass, after a fine calibration of the ellipsometre with the reference Silica glass over the spectral range between 0.260 μm to 2 μm thanks to the comparison to literature. This allowed estimating the dispersion behavior of this glass, especially between the 1.030 μm fundamental beam and the THG radiation at 0.343 μm . The preparation of a 1 mm thick sample with a low surface roughness and slightly wedged permitted to consider it as a bulk material. Hence, the refractive indices were directly retrieved with an accuracy better than 0.01, leading to the $\chi^{(3)}$ estimation with 22% uncertainty.

3. Results and discussion

The glass (in cation mol. %) 40 GaO_{3/2} - 26.4 GeO₂ - 16.4 BaO - 8.6 LaO_{3/2} - 8.6 YO_{3/2} (namely GGBLaY) was selected for the present study. Measurements of the thermal properties, refractive

index dispersion, Raman gain cross section, third order susceptibility, optical transmission as well as Knoop micro-hardness were performed in order to fully grasp the potential of the GGBLaY glass for photonic applications in the Mid-IR. The glass properties are summarized in **Table 1** and compared to the main existing infrared materials.

Table 1. Physical properties of Infrared transmitting glasses, namely glass transition temperature (T_g), Third order susceptibility ($\chi^{(3)}$), Raman gain cross-section (g_R) and Knoop micro-hardness (H_K).

Glass	Main component	T_g (°C)	Transmission window (μm)	$\chi^{(3)}$ ($\times 10^{-22}$ m ² V ⁻²) ^{a)}	g_R ($\times 10^{-13}$ m W ⁻¹)	H_K (GPa)
Silica [3,16,17]	SiO ₂	1250	0.19 - 4.0	2	0.9	5.9
Gallate	Ga₂O₃	735	0.28 - 6.0	28	5.4	5.4
Germanate [3,18–23]	GeO ₂	500 ^b - 700 ^c	0.28 - 5.5 ^b	~3 ^d - 25 ^b	~4 ^d - 15 ^b	3.9 ^b - 5.1 ^d
Tellurite [3,14,24]	TeO ₂ - ZnO	260 - 370	0.4 - 6.5	74	20	2.9–3.3
Fluoride [3,14,17,25]	ZrF ₄ - BaF ₂	260	0.2 - 8.0	2.6	2	2.2
Chalcogenide [3,4,26]	As ₂ S ₃	230	0.55 - 12.0	1251	44	1.1–2.0

^aCalculated from n_0 and n_2 values given in literature at 1.06 μm for silica, germanates, tellurites and fluorides and at 1.55 μm for As₂S₃ [3,19,21]

^bFor GeO₂ – PbO glasses with GeO₂ content > 40 mol. % [23,26]

^cFor BaO – GeO₂ – Ga₂O₃ glasses with GeO₂ content > 40 mol. % [18]

^dFor lead-free GeO₂ – SiO₂ glasses with GeO₂ content > 40 mol. % [19,20]; (for estimation of optical window the material thickness are the following: Silica: 2 mm, gallate: 2 mm, germanate: 12 mm, tellurite: 1 mm, fluoride: 2 mm, chalcogenide: 3 mm)

The characteristic temperatures of the glass, namely the glass transition (T_g) and crystallization onset temperatures (T_x), were determined in a previous study through differential thermal analysis [27]. The T_g is found to be 735 °C while the onset of the first crystallization peak appears $T_x = 910$ °C. Because of its high T_g , the present composition can be considered for the design of devices operating in harsh environments with elevated temperatures or to sustain the heat effects occurring during high power Laser operations for instance. Additionally, the glass possesses a high difference ΔT value between T_x and T_g ($\Delta T = T_x - T_g = 175$ °C), which gives GGBLaY fibers practical advantages for its splice-based integration into all-fiber architectures where connections to important components such as pump sources, isolators, Bragg gratings and others, are necessary. Functionalization of the fiber (end-capping, tapering, lensing, etc.) can also be considered in this instance without risking recrystallizations of the glass during temperature-based post-processing steps.

The refractive index dispersion curve of the present gallate glass is given in **Fig. 1**. It exhibits a typical normal dispersion with a decrease of the refractive index versus the wavelength. The refractive index is 1.778 ± 0.01 at 1.550 μm. Fine refractive index is of great importance for the development of complex fiber structures suitable for photonic applications. It allows for the engineering of waveguiding properties as well as the excitation of specific nonlinear dynamics through dispersion management and light confinement. In the present case, modulation of the refractive index can be achieved by tailoring for instance the Ga₂O₃ content in the glass offering very versatile possibilities for fiber developments. Indeed, waveguides with different index steps can be built from those easily tunable compositions and depending on the application, single-mode fibers with either large mode area (LMA) can be targeted for laser operation or on the contrary, fibers with small effective area can be produced as they are more profitable for the triggering of particular nonlinear effects. For refractive index engineering, precise measurements will be needed on fibers to estimate the refractive index profile, involving for instance interferometry methods to reach the necessary accuracy.

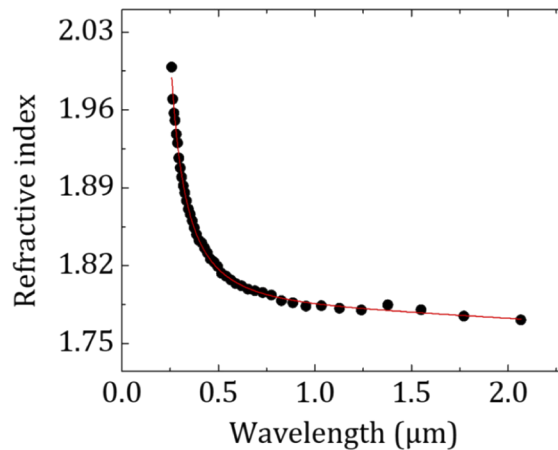


Fig. 1. Refractive index dispersion of the GGBLaY glass.

The third order susceptibility and the Raman gain cross section were measured to confirm the great potential of high Ga_2O_3 content materials as promising candidates for the next generation of nonlinear photonic devices in the spectral region covering the transition between NIR and Mid-IR. The third order susceptibility value was determined through third harmonic generation (THG) measurements at $0.343 \mu\text{m}$. An IR laser emitting at $1.030 \mu\text{m}$ was used to ensure a non-resonant configuration measurement in the transparency window of the glass matrix while taking into account the refractive index dispersion presented further below.

The third harmonic measurement, as compared to Kerr effect measurement for instance, allows accessing mainly to the electronic contribution of the nonlinear response. It permits in particular to avoid a possible nuclear contribution to a nonlinear index measurement as it has been reported for germanium containing silicate or niobium containing phosphate glasses in which, the nuclear contribution to the n_2 can reach 40% depending on the pulse laser duration and the pump probe measurement configuration [35,36]. The $\chi^{(3)}$ values as function of the linear refractive index for various materials, namely silicates, germanates containing heavy oxides, fluorides, borophosphates, phosphates, tellurites, chalcogenides and some simple oxides are plotted in **Fig. 2** [3,19,21,28–34]. For the GGBLaY glass, the $\chi^{(3)}$ values measured by THG is $2.8 \times 10^{-21} \text{ m}^2 \text{ V}^{-2}$ which is approximately one order magnitude stronger than for SiO_2 . The value is above the reported ones for germanates. There are only few studies concerning nonlinear optical properties of gallium oxide containing glasses beside materials with lead or bismuth in which the property is mainly driven by those latter anions. Nonetheless, since there is correlation of the nonlinear optical properties with the linear refractive index, one can have information about the effect of gallium oxide from the linear optical responses of gallate glasses for which the literature is more extensive. Indeed, as previously measured, the gallium oxide when associated to germanium oxide contributes to the increase of the linear refractive index of glasses [37]. Similar effect is also observed in the case of alkali and alkaline earth gallo-silicate glass, where the introduction of gallium in the germanate glass network leads to the formation of GaO_4 tetrahedra where the alkali and the alkaline earth ions act first as charge compensator ions leading to limited amount of polarizable Ge-O-Na bonds called NBO (non-bridging oxygen). Such NBO bonds on germanium or silicon are expected to exist only after the fourfold coordinated gallium ions has consumed the equivalent amount of modifier ions to form GaO_4 [38,39]. In the GGBLaY composition, the glass network is composed of connected GeO_4 and GaO_4 units surrounded by alkaline earth or rare earth ions acting as charge compensators. This yields a dense glass network with increased density as compared to germanate matrices, despite the fact that the molar weight

of gallium and germanium are comparable [40]. Such effect is most probably at the origin of the largest linear and nonlinear response of the gallium containing glasses as compared to germanate. Such effect was previously proposed by Line, who claimed in early 1991 that gallate glass matrices could be promising for nonlinear optical applications, despite the few investigations that had been reported concerning those materials at that time [41].

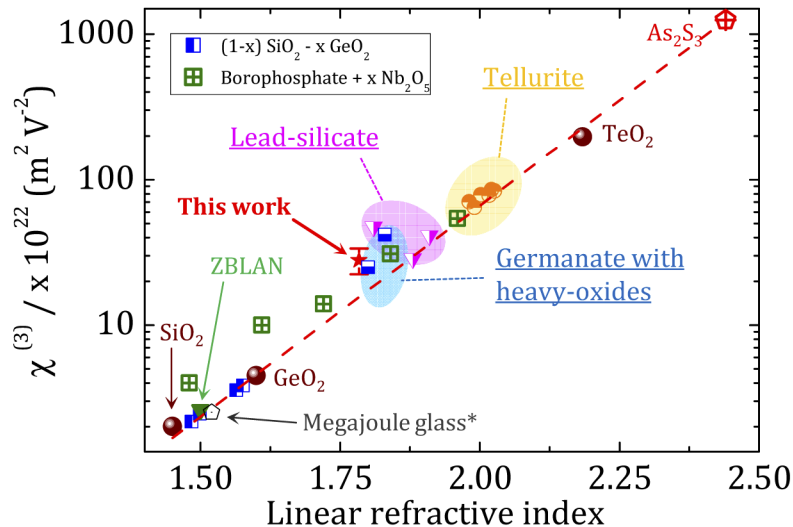


Fig. 2. $\chi^{(3)}$ values as function of the linear refractive index for various glass families. Values were either directly extracted from literature or calculated from available n_0 and n_2 values [3,19,21,28–33]. *Megajoule Glass: Phosphate glass amplifier designed for the French Mégajoule Laser ignition facilities [34].

The Raman gain spectral response of the GGBLaY glass is plotted in **Fig. 3** and is compared to SiO_2 . It exhibits two main vibration modes centered at 525 cm^{-1} and 800 cm^{-1} . The band around 525 cm^{-1} can be attributed to the mixed symmetric stretching and bending vibrations of T–O–T bridges with T = Ge or Ga. Regarding the broad band around 800 cm^{-1} , the assignment is either germanium non-bridging oxygen or antisymmetric vibration of T–O–T bridges [39,42]. Indeed, as detailed in [39] which combines DFT calculations with IR and Raman characterizations of gallo-germanate glasses, we attribute the non-uniform charge repartition on oxygen ions along the gallo-germanate chains (as expected with the $[\text{GaO}_4]^-$ tetrahedra charge compensated by neighboring barium, yttrium or lanthanum ions) to be responsible for the intense vibration between 650 cm^{-1} and 900 cm^{-1} also observed using infrared spectroscopy [39]. One has to note that the maximum Raman cross section of such gallium-rich glass system is ~ 5.4 times stronger than the fused silica one, outranking fluorides (~ 2.2 times silica for ZBLAN [14,17]) as well as common germanate materials (~ 4.5 times silica for lead-free GeO_2 glasses [9]). Such value has to be related again to the germano-gallate glass network structure favoring high density T-O-T network with inhomogeneous charge distribution on oxygen atoms and part of the barium, yttrium and lanthanum ions acting as charge compensators for GaO_4 tetrahedra.

Optical transmission of the GGBLaY bulk glass is shown on **Fig. 4(a)**. The transmission window for a sample of 2 mm in thickness spans from $\sim 0.280 \mu\text{m}$ up to $\sim 6.0 \mu\text{m}$ in the Mid-IR. One can observe a significant absorption at $3.0 \mu\text{m}$ usually attributed to free T-OH groups (with T used for Ga or Ge) or molecular water traditionally measured on glass prepared with no special purification steps [43,44]. Attenuation measurements were performed on optical fiber samples by the cutback technique in the visible and Near Infrared spectral range, between $0.400 \mu\text{m}$ and $2.4 \mu\text{m}$. As a comparison, the same measurement was conducted using a discrete laser wavelength

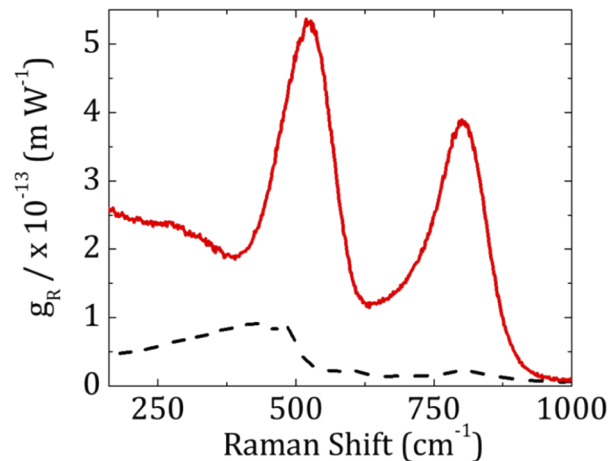


Fig. 3. Raman gain cross section of the GGBLaY glass (red line) compared to silica (black line)

at 1.310 μm . The results are summarized on **Fig. 4(b)**. They reveal a typical transmission of a fiber made from unpurified heavy-oxide glass. The background loss level is ~ 6 dB/m and the transmission is limited towards longer wavelengths by strong water-related absorptions usually attributed to harmonics of bonded-hydroxyl or free H_2O vibrations [44]. One has to keep in mind that the viscosity of the melt is particularly high, making difficult the homogenization and the casting operations. The preform and the fiber presented visible striae as observed in the insert of Fig. 4(b). Regarding impurities, the synthesis under dry atmosphere and addition of dehydration reagents to the melt (halides like ZnF_2 , BaF_2 , etc.) should allow to effectively remove water-related impurities from the glass and extend the optical transmission in the Mid-IR [13,45] and would widen the fiber transmission to ~ 4.5 μm in the IR. Opening the important 3–5 μm window would allow for the development of sources based on rare-earth Mid-IR emissions from, for instance, Er^{3+} , Ho^{3+} , Pr^{3+} and Dy^{3+} ions. Gallate matrices possess high RE-ions solubility, as reported in literature [46], and as confirmed by the high amount of lanthanide and yttrium oxides (17 mol. % of $\text{YO}_{3/2} + \text{LaO}_{3/2}$) already incorporated in the present GGBLaY composition. This ability to integrate a large amount of RE-ions makes gallate glasses attractive for the design of high power, extremely short laser configurations. Additionally, the present composition does not contain alkali ions which are known to be responsible for color centers formation in glasses. It is worth noting that the GGBLaY fiber keeps good transmission at lower wavelengths down to 0.5 μm , meaning that those glasses possess great potential for applications both in the visible and Mid-IR spectral domains.

Mechanical strength was also assessed through Knoop indentation measurements. The surface micro-hardness of the glass sample was found to be 5.4 ± 0.3 GPa which confirms the improved mechanical properties of gallium rich glasses. This value, despite remaining lower than that of silica (5.9 GPa [16]), is greater than those exhibited by all other IR materials such as chalcogenides (1.1 GPa for As_2S_3 [26]), fluorides (2.2 GPa for ZBLAN [25]) and tellurides (2.5 GPa or slightly more depending on network modifier [24,47]). The germanate family places just below with almost similar mechanical toughness but lesser Raman gain cross section and third order susceptibility as described previously in Table 1. One can note that GeO_2 -PbO or BGG glasses, which are the most profitable germanium oxide-based materials in terms of IR transmission and nonlinear responses, exhibit lower surface hardness (respectively 3.9 GPa and 4.1 GPa [18,23]).

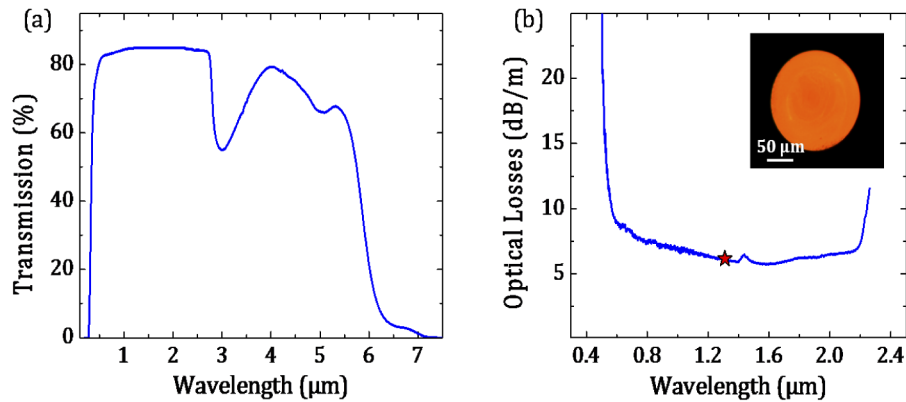


Fig. 4. (a) Transmission spectra recorded for a 2 mm bulk GGBLaY glass. (b) Optical attenuation of the glass fiber measured between 0.400 μm and 2.400 μm. A discrete loss measurement performed with a laser source at 1.310 μm was added to the graph (red star). Inset: Cross-sectional view of a mono-material gallate fiber.

Regarding $\text{GeO}_2\text{-SiO}_2$ and $\text{GeO}_2\text{-Al}_2\text{O}_3$ systems, they show improved mechanical properties (with surface hardness over 4.9 GPa [49]) but with reduced transmission in the Mid-IR or weaker $\chi^{(3)}$ and Raman gain. In order to increase nonlinear responses in those glasses, germanium oxide content has to be risen [19,20], leading to lower chemical durability and poor optical quality. In the end, for germanate matrices as opposed to gallate glasses, mechanical strength usually has to be traded for either extension of the IR transmission or improvement of the nonlinear responses. To emphasize the potential of gallium-rich glasses, Knoop micro-hardness of the existing IR vitreous families versus their IR transmission edge is plotted in **Fig. 5**. For most of the available glass families reported, their surface hardness decreases with the extension of their IR transmission edge. Following this tendency, they can be organized in the following order: silicates, germanates, tellurites, fluorides and finally chalcogenides. Gallate glasses however do

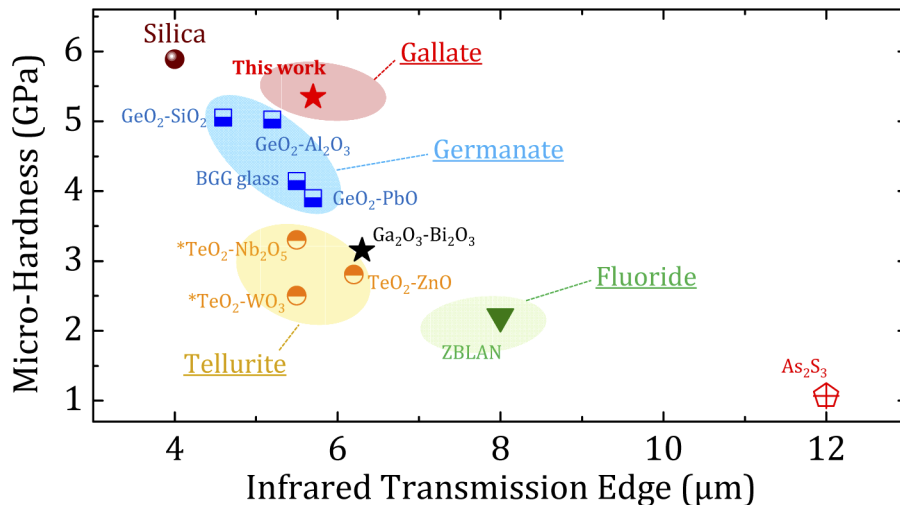


Fig. 5. Knoop Micro-hardness measured of the available Infrared glass materials as function of their transmission edge at longer wavelengths [16,18,23–26,47–49]. Compositions marked with an asterisk refer to values measured with a Vickers indenter [47].

not fall in this classification and keep high surface hardness with a moderate transmission limit at longer wavelengths reaching nearly 6 μm . In this context, Ga_2O_3 -based materials offer a new alternative for the development of highly robust fiber-based photonic devices exploiting either linear (RE emissions) or nonlinear processes (Kerr effect, Raman gain, etc.) and potentially able to operate in the visible up to the Mid-IR range.

4. Conclusion

Gallium-rich gallo-germanate glasses incontestably appear here as a serious alternative to silica, as they uniquely combine reinforced thermal and mechanical properties, fiber-drawing ability, high rare earth ions solubility. Such glass compositions offer a wide transmission window with transmission expected to reach 4.5 μm in fiber. They exhibit the highest nonlinear optical responses among the friendly oxide glass compositions. However for the deployment of such glass, the main target remains in term of synthesis conditions to reach minimal optical losses ($\sim 1 \text{ dB}\cdot\text{km}^{-1}$) in the IR. Then it would lead to a new level of robust fiber laser sources and innovative fiber components for manipulating light, with applications spanning important areas, such as communication technology, metrology or sensing. Sources based on these materials will allow increasing the output power as compared to existing devices, especially in the Mid-IR, enabling the development of novel robust, more reliable, high energy photonic systems.

Funding. Centre National de la Recherche Scientifique (LIA LuMAQ); H2020 Marie Skłodowska-Curie Actions (823941); Fonds de recherche du Québec – Nature et technologies; Canada Excellence Research Chairs, Government of Canada; Natural Sciences and Engineering Research Council of Canada; Conseil Régional Aquitaine; Agence Nationale de la Recherche (17-CE08-0042-01, ANR-10-IDEX-03-02).

Acknowledgements. This research was supported by the Canadian Excellence Research Chair program (CERC) in Photonics Innovations, the Natural Sciences and Engineering Research Council of Canada (NSERC), the Agence Nationale de la Recherche (ANR) (ANR-17-CE08-0042-01), the CNRS (LIA LuMAQ) and the New Aquitaine Region. This project has received funding from the European Union's Horizon 2020 research and innovation program under the Marie Skłodowska-Curie grant agreement No 823941 (FUNGLASS). The authors are also grateful to the Fonds de Recherche Québécois sur la Nature et les Technologies (FRQNT) and the Canadian Foundation for Innovation (CFI) for the financial support. Mobilities were supported by grants of the French Consulate in Québec (by the Frontenac Program), the association of Campus France and Mitacs Globalink as well as grants of the Agence Nationale de la Recherche (ANR) with the program "Investissement d'avenir" number ANR-10-IDEX-03-02.

Disclosures. The authors declare no conflicts of interest.

References

1. G. Tao, H. Ebendorff-Heidepriem, A. M. Stolyarov, S. Danto, J. V Badding, Y. Fink, J. Ballato, and A. F. Abouraddy, "Infrared fibers," *Adv. Opt. Photonics* **7**(2), 379–458 (2015).
2. H. Bach and N. Neuroth, *The Properties of Optical Glass* (Springer Science & Business Media, 2012).
3. J. H. V Price, T. M. Monro, F. Ebendorff-Heidepriem Heikeand Poletti, P. Horak, V. Finazzi, J. Y. Y. Leong, P. Petropoulos, J. G. Flanagan, and C. Brambilla, "Mid-IR supercontinuum generation from nonsilica microstructured optical fibers," *IEEE J. Select. Topics Quantum Electron.* **13**(3), 738–749 (2007).
4. M. Asobe, T. Kanamori, K. Naganuma, H. Itoh, and T. Kaino, "Third-order nonlinear spectroscopy in As_2S_3 chalcogenide glass fibers," *J. Appl. Phys.* **77**(11), 5518–5523 (1995).
5. Z. Zheng, D. Ouyang, J. Zhao, M. Liu, S. Ruan, P. Yan, and J. Wang, "Scaling all-fiber mid-infrared supercontinuum up to 10 W-level based on thermal-spliced silica fiber and ZBLAN fiber," *Photonics Res.* **4**(4), 135 (2016).
6. Y. O. Aydin, F. Maes, V. Fortin, S. T. Bah, R. Vallée, and M. Bernier, "Endcapping of high-power 3 μm fiber lasers," *Opt. Express* **27**(15), 20659 (2019).
7. S. S. Bayya, J. S. Sanghera, and I. D. Aggarwal, Optical transmission of BGG glass material, patent US7285509B2 (2004).
8. P. L. Higby and I. D. Aggarwal, "Properties of barium gallium germanate glasses," *J. Non-Cryst. Solids* **163**(3), 303–308 (1993).
9. S. S. Bayya, B. B. Harbison, J. S. Sanghera, and I. D. Aggarwal, " $\text{BaO-Ga}_2\text{O}_3\text{-GeO}_2$ glasses with enhanced properties," *J. Non-Cryst. Solids* **212**(2-3), 198–207 (1997).
10. X. Wen, G. Tang, Q. Yang, X. Chen, Q. Qian, Q. Zhang, and Z. Yang, "Highly Tm^{3+} doped germanate glass and its single mode fiber for 2.0 μm laser," *Sci. Rep.* **6**, 20344 (2016).
11. X. Wen, G. Tang, J. Wang, X. Chen, Q. Qian, and Z. Yang, " Tm^{3+} doped barium gallo-germanate glass single-mode fibers for 20 μm laser," *Opt. Express* **23**(6), 7722 (2015).

12. K. Yoshimoto, A. Masuno, M. Ueda, H. Inoue, H. Yamamoto, and T. Kawashima, "Low phonon energies and wideband optical windows of $\text{La}_2\text{O}_3\text{-Ga}_2\text{O}_3$ glasses prepared using an aerodynamic levitation technique," *Sci. Rep.* **7**(1), 45600 (2017).
13. J. Chung, Y. Watanabe, Y. Yananba, Y. Nakatsuka, and H. Inoue, "Novel gallate-based oxide and oxyfluoride glasses with wide transparency, high refractive indices, and low dispersions," *J. Am. Ceram. Soc.* **103**(1), 167–175 (2020).
14. M. D. O'Donnell, K. Richardson, R. Stolen, C. Rivero, T. Cardinal, M. Couzi, D. Furniss, and A. B. Seddon, "Raman gain of selected tellurite glasses for IR fibre lasers calculated from spontaneous scattering spectra," *Opt. Mater.* **30**(6), 946–951 (2008).
15. A. Royon, B. Bousquet, L. Canioni, M. Treguer, T. Cardinal, E. Fargin, D.-G. Kim, and S.-H. Park, "Third-harmonic generation microscopy for material characterization," *J. Opt. Soc. Korea* **10**(4), 188–195 (2006).
16. G. D. Quinn, P. Green, and K. Xu, "Cracking and the indentation size effect for Knoop hardness of glasses," *J. Am. Ceram. Soc.* **86**(3), 441–448 (2003).
17. T. Mizunami, H. Iwashita, and K. Takagi, "Gain saturation characteristics of Raman amplification in silica and fluoride glass optical fibers," *Opt. Commun.* **97**(1-2), 74–78 (1993).
18. S. S. Bayya, G. D. Chin, J. S. Sanghera, and I. D. Aggarwal, "Germanate glass as a window for high energy laser systems," *Opt. Express* **14**(24), 11687 (2006).
19. Y. Yatsenko and A. Mavritsky, "D-scan measurement of nonlinear refractive index in fibers heavily doped with GeO_2 ," *Opt. Lett.* **32**(22), 3257 (2007).
20. S. T. Davey, D. L. Williams, B. J. Ainslie, W. J. M. Rothwell, and B. Wakefield, "Optical gain spectrum of $\text{GeO}_2\text{-SiO}_2$ Raman fibre amplifiers," *IEE Proc.-J: Optoelectron.* **136**(6), 301 (1989).
21. Y. Y. Huang, A. Sarkar, and P. C. Schultz, "Relationship between composition, density and refractive index for germania silica glasses," *J. Non-Cryst. Solids* **27**(1), 29–37 (1978).
22. A. E. Miller, K. Nassau, K. B. Lyons, and M. E. Lines, "The intensity of Raman scattering in glasses containing heavy metal oxides," *J. Non-Cryst. Solids* **99**(2-3), 289–307 (1988).
23. S. Gao, X. Fan, X. Liu, M. Liao, and L. Hu, "Mechanical and $\sim 2\ \mu\text{m}$ emission properties of Tm^{3+} -doped $\text{GeO}_2\text{-TeO}_2$ (or SiO_2)- PbO-CaO glasses," *Opt. Mater.* **45**, 167–170 (2015).
24. S. Yoshida, S. Aono, J. Matsuoka, and N. Soga, "Indentation behavior of zinc tellurite glasses by using a Knoop indenter," *J. Ceram. Soc. Japan* **109**(1273), 753–756 (2001).
25. T. Iqbal, M. R. Shahriari, G. Merberg, and G. H. Sigel, "Synthesis, characterization, and potential application of highly chemically durable glasses based on AlF_3 ," *J. Mater. Res.* **6**(2), 401–406 (1991).
26. J. S. Sanghera, L. B. Shaw, and I. D. Aggarwal, "Applications of chalcogenide glass optical fibers," *Comptes Rendus Chim.* **5**(12), 873–883 (2002).
27. T. Guérineau, C. Strutyński, T. Skopak, S. Morency, A. Hanafi, F. Calzavara, Y. Ledemi, S. Danto, T. Cardinal, Y. Messaddeq, and E. Fargin, "Extended germano-gallate fiber drawing domain: from germanates to gallates optical fibers," *Opt. Mater. Express* **9**(6), 2437 (2019).
28. T. Cardinal, E. Fargin, G. Le Flem, and S. Leboiteux, "Correlations between structural properties of $\text{Nb}_2\text{O}_5\text{-NaPO}_3\text{-Na}_2\text{B}_4\text{O}_7$ glasses and non-linear optical activities," *J. Non-Cryst. Solids* **222**, 228–234 (1997).
29. S.-H. Kim, T. Yoko, and S. Sakka, "Linear and nonlinear optical properties of TeO_2 glass," *J. Am. Ceram. Soc.* **76**(10), 2486–2490 (1993).
30. V. Dimitrov and T. Komatsu, "Classification of oxide glasses: a polarizability approach," *J. Solid State Chem.* **178**(3), 831–846 (2005).
31. S. Manning, H. Ebdorff-Heidepriem, and T. M. Monro, "Ternary tellurite glasses for the fabrication of nonlinear optical fibres," *Opt. Mater. Express* **2**(2), 140 (2012).
32. H. Nasu, J. Matsuoka, O. Sugimoto, M. Kida, and K. Kamiya, "Non-resonant type third-order optical nonlinearity of rare earth oxides-containing GeO_2 glasses," *J. Ceram. Soc. Japan* **101**(1169), 43–47 (1993).
33. D. W. Hall, M. A. Newhouse, N. F. Borrelli, W. H. Dumbaugh, and D. L. Weidman, "Nonlinear optical susceptibilities of high-index glasses," *Appl. Phys. Lett.* **54**(14), 1293–1295 (1989).
34. J. H. Campbell, T. I. Suratwala, C. B. Thorsness, J. S. Hayden, A. J. Thorne, J. M. Cimino, A. J. Marker Iii, K. Takeuchi, M. Smolley, and G. F. Ficini-Dorn, "Continuous melting of phosphate laser glasses," *J. Non-Cryst. Solids* **263-264**, 342–357 (2000).
35. S. Smolorz and F. Wise, "Measurement of the nonlinear optical response of optical fiber materials by use of spectrally resolved two-beam coupling," *Opt. Lett.* **24**(16), 1103–1105 (1999).
36. A. Royon, L. Canioni, B. Bousquet, V. Rodriguez, M. Couzi, C. Rivero, T. Cardinal, E. Fargin, M. Richardson, and K. Richardson, "Strong nuclear contribution to the optical Kerr effect in niobium oxide containing glasses," *Conference on Lasers and Electro-Optics (CLEO)* **2007**, 1–6 (2007).
37. T. Skopak, P. Hee, Y. Ledemi, M. Dussauze, S. Kroeker, T. Cardinal, E. Fargin, and Y. Messaddeq, "Mixture experimental design applied to gallium-rich," *J. Non-Crystall. Solids* **455**, 83–89 (2017).
38. H. Doweidar, "Optical properties and structure of $\text{R}_2\text{O-Ga}_2\text{O}_3\text{-SiO}_2$ and $\text{RO-Ga}_2\text{O}_3\text{-SiO}_2$ glasses," *J. Mater. Sci.* **44**(11), 2899–2906 (2009).
39. T. Skopak, S. Kroeker, K. Levin, M. Dussauze, R. Méreau, Y. Ledemi, T. Cardinal, E. Fargin, Y. Messaddeq, T. Skopak, S. Kroeker, K. Levin, M. Dussauze, R. Me, E. Fargin, and Y. Messaddeq, "Structure and properties of gallium-rich sodium germano-gallate glasses," *J. Phys. Chem. C* **123**(2), 1370–1378 (2019).

40. N. Cezard, A. Dobroc, G. Canat, M. Duhant, W. Renard, C. Alhenc-Gelas, S. Lefebvre, and J. Fade, "Supercontinuum laser absorption spectroscopy in the mid-infrared range for identification and concentration estimation of a multi-component atmospheric gas mixture," in *SPIE Remote Sensing* (2011), pp. 81820V.
41. M. E. Lines, "Oxide glasses for fast photonic switching: a comparative study," *J. Appl. Phys.* **69**(10), 6876–6884 (1991).
42. T. Furukawa and W. B. White, "Raman spectroscopic investigation of the structure and crystallization of binary alkali germanate glasses," *J. Mater. Sci.* **15**(7), 1648–1662 (1980).
43. F. Ernsberger, "Molecular water in glass," *J. Am. Ceram. Soc.* **60**(1-2), 91–92 (1977).
44. M. D. O'Donnell, C. A. Miller, D. Furniss, V. K. Tikhomirov, and A. B. Seddon, "Fluorotellurite glasses with improved mid-infrared transmission," *J. Non-Cryst. Solids* **331**(1-3), 48–57 (2003).
45. J. Massera, A. Haldeman, J. Jackson, C. Rivero-Baleine, L. Petit, and K. Richardson, "Processing of tellurite-based glass with low OH content," *J. Am. Ceram. Soc.* **94**(1), 130–136 (2011).
46. M. Boyer, A. J. F. Carrion, S. Ory, A. I. Becerro, S. Villette, S. V. Eliseeva, S. Petoud, P. Aballea, G. Matzen, and M. Allix, "Transparent polycrystalline Sr: RE Ga₃O₇ melilite ceramics: potential phosphors for tuneable solid state lighting," *J. Mater. Chem. C* **4**(15), 3238–3247 (2016).
47. R. A. H. El-Mallawany, *Tellurite Glasses Handbook* (CRC Press, 2016).
48. L. R. P. Kassab, L. C. Courrol, N. U. Wetter, S. H. Tatumi, and C. M. S. P. Mendes, "Glasses of heavy metal and gallium oxides doped with neodymium," *Radiat. Eff. Defects Solids* **156**(1-4), 371–375 (2001).
49. W. H. Dumbaugh, "Infrared transmitting glasses," *Opt. Eng.* **24**(2), 242257 (1985).